16 Apr 1992

Solution of Divertor Magnetohydrodynamic Equilibria for the Study of Alpha Particle Edge Transport in Fusion Plasmas

J. W. Schumer

SOLUTION OF DIVERTOR MAGNETOHYDRODYNAMIC EQUILIBRIA FOR THE STUDY OF ALPHA PARTICLE EDGE TRANSPORT IN FUSION PLASMAS

by J. W. Schumer
Nuclear Engineering

ABSTRACT

Removal of thermalized alpha particles from deuterium-tritium (D-T) fusion plasmas can be accomplished through the use of divertor magnetic fields if the magnetohydrodynamic (MHD) equilibria is well understood [1]. Modifying a MHD variational energy principle for poloidal flux surfaces described by $\chi = \chi(\rho,\theta)$ results in an inverse Fourier representation of the three-dimensional (3-D) equilibria solution. Application of the $\chi(\rho,\theta)$ flux profile allows transformation of the magnetic field into a non-singular coordinate system along the divertor separatrix [2] and therefore, analysis of different divertor schemes. Derivation of the coupled, non-linear differential equations follows [5] except in the contravariant representation of the magnetic field. Theoretical background, formulation of the variational principle, benchmark results, and preliminary computations are presented.

INTRODUCTION

Transport, accumulation, and thermalization of alpha particles in a deuterium-tritium (D-T) plasma are critical phenomena which may preclude sustained ignition in a fusion reactor. Alpha particles are produced by the D-T reaction [1],

$$ {}_1^2D + {}_1^3T \rightarrow {}_0^1n(14.1\ MeV) + {}_2^4He(3.52\ MeV) \qquad (1) $$

releasing 2.818E-12 J/reaction for continued ignition of the plasma. Unfortunately, non-classical transport or containment of thermalized helium ash (low energy population of alphas) could quench the fusion reaction [1,4]. Removal of helium ash may be accomplished using a poloidal divertor (see Figure 1) to scrape the plasma edge if ash distributions are fairly flat and if the resulting perturbation of magnetohydrodynamic (MHD) equilibrium is well understood.

This research involved the enhancement of VMEC (Variational Moments Equilibrium Code [5,6,7,8]), allowing it to solve the high-β MHD equilibria equations associated with a divertor magnetic separatrix. The separatrix is the bounding surface between open and closed field lines [2] (see Figure 2) and equilibrium calculations are simplest when using magnetic coordinates $\alpha(\rho,\theta,\zeta)$ in which the contravariant form of the magnetic field is defined,

$$\vec{B} = \nabla\phi\times\nabla\theta - \nabla\chi(\phi)\times\nabla\zeta \qquad (2)$$

where ϕ is the toroidal flux, ζ is the toroidal angle, χ is the poloidal flux, and θ is the poloidal angle. However, this form is mathematically singular along the separatrix because the helical flux $\chi_h(\psi)$ is a function of toroidal flux alone and the toroidal flux ψ goes to infinity along the separatrix. Recent progress [3] has revealed a transformation to nonmagnetic coordinates which preserves some of the attractive features of magnetic coordinates while removing their discontinuous nature. By retaining the helical flux in the contravariant form of the magnetic field, defined as

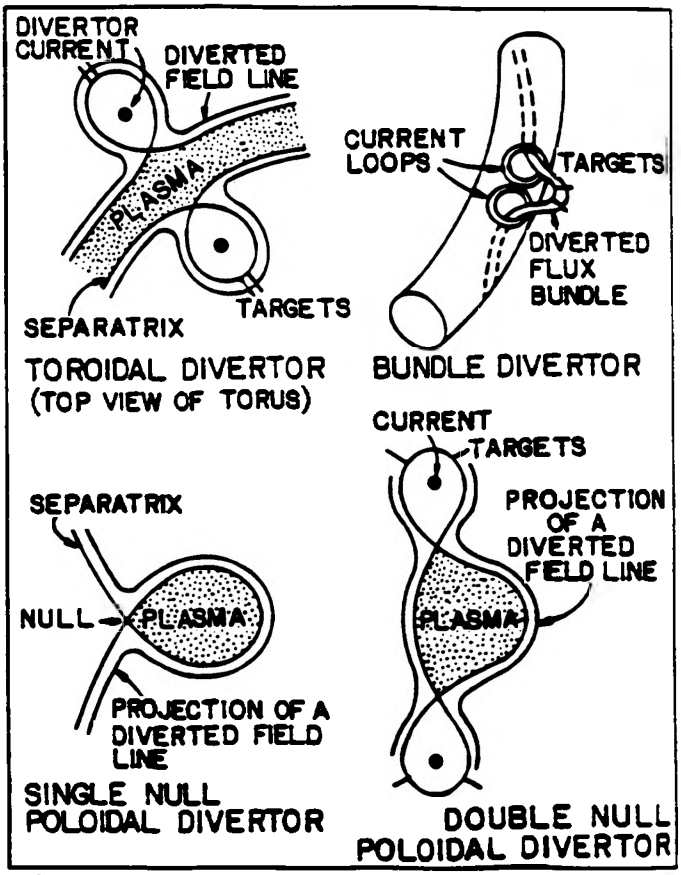

Figure 1. Toroidal, poloidal, and bundle divertors (from Dolan, 729).

$$\vec{B} = \nabla\phi\times\nabla\theta - \nabla\chi(\rho,\theta)\times\nabla\zeta \qquad (3)$$

allows for the modification of the variational moments MHD energy principle in VMEC and the production of an efficient, finite-series representation for the three-dimensional (3-D) plasma boundary with a separatrix.

ANALYTICAL DERIVATIONS

Magnetic field

Generally, Equation (3) is the form of the magnetic field

used for solution of force-balance equation $\vec{F} = -\vec{J}\times\vec{B} + \nabla p = 0$, where F is the residual force vanishing at equilibrium and p is the pressure on the radial flux surface labeled by ρ. However, to aid in the convergence of the inverse Fourier series representation used in VMEC, the renormalization parameter λ is introduced, allowing for distinction between geometric and magnetic angles [6]. The renormalization parameter is a function of the three magnetic coordinates $\alpha(\rho,\theta,\zeta)$ and is used in linear combination with one of the cylindrical coordinates normally visualized with fusion toroidal devices (see Figure 3). Unfortunately, implementation of this parameter with the poloidal angle does not allow for conservation of the magnetic field along flux surfaces. However, using λ with the toroidal angle satisfies $\vec{B}\cdot\nabla\chi(\rho,\theta) = 0$ *when* $\zeta^* = \zeta \pm \lambda$ and results in the following contravariant magnetic representation:

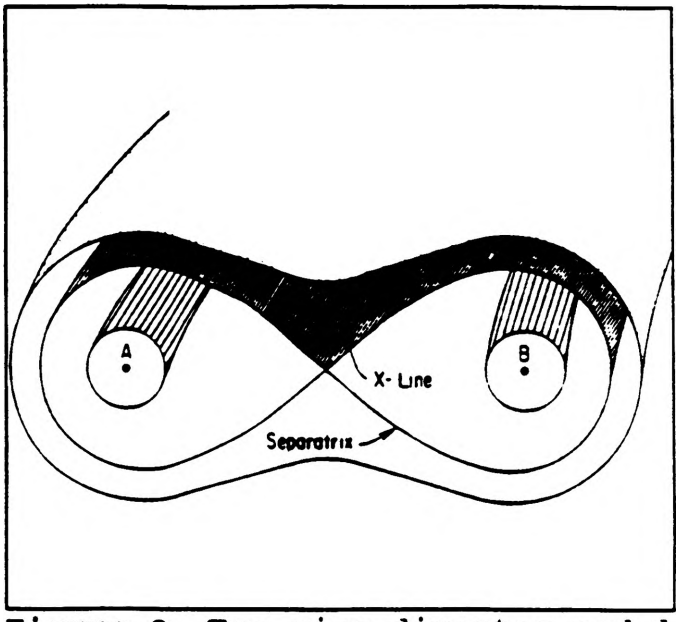

Figure 2. Two-wire divertor model illustrating separatrix and X-line (Boozer, 2398).

$$\vec{B} = \nabla\phi\times\nabla\theta - \nabla\chi\times\nabla\zeta \pm \nabla\chi\times\nabla\lambda \ . \tag{4}$$

Taking the dot product of (4) with its covariant basis vectors $\nabla\alpha_i$ *where* $\alpha = (\rho,\theta,\zeta)$ [10], the contravariant components of $\vec{B}$ are

$$B^\rho = -\frac{\chi_\theta}{\sqrt{g}}(1 - \lambda_\rho) \tag{5a}$$

$$B^\theta = \frac{\chi_\rho}{\sqrt{g}}(1 - \lambda_\rho) \tag{5b}$$

$$B^\zeta = \frac{1}{\sqrt{g}}(\phi_\rho + \chi_\rho\lambda_\theta + \chi_\theta\lambda_\rho) \tag{5c}$$

where $\sqrt{g} = (\nabla\rho\cdot\nabla\theta\times\nabla\zeta)^{-1}$ is the Jacobian. These results will be used in the derivation of energy principle.

Variational Principle

The variational principle used for the solution of the equilibrium is based on the plasma energy

$$W = \int \left(\frac{|B|^2}{2\mu_o} + \frac{p}{(\gamma - 1)} \right) d^3x \quad (6)$$

where $d^3x = x(R,\phi,Z)$ is the Cartesian coordinate system and $\gamma > 0$ is the adiabatic index. By taking the inverse representation, for which $\alpha = \alpha(x) = \alpha(\rho,\theta,\zeta)$, the mass and flux are conserved in the contravariant representation of B. Differentiating (6) and integrating by parts, the spatial differentials are separated into a steepest-descent formulation for the F=0 solution of MHD force equation that preserves finite positive energy, such that

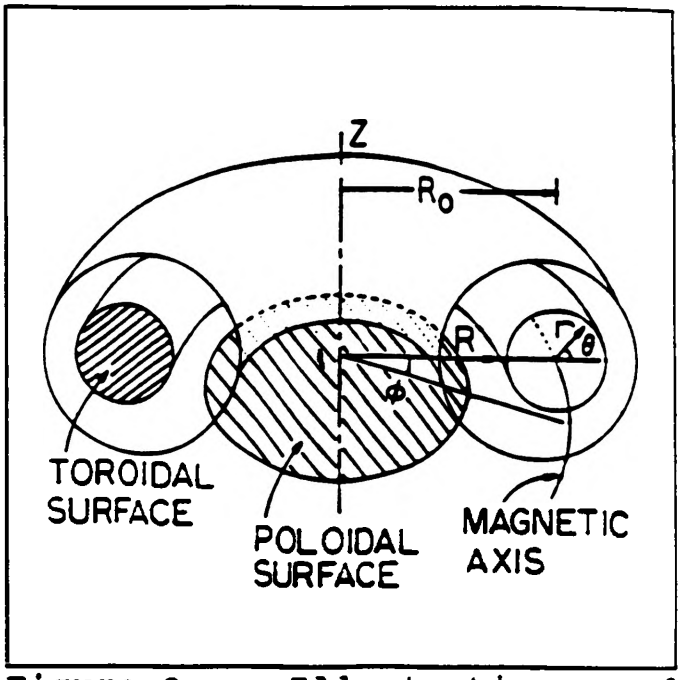

Figure 3. Illustration of toroidal and poloidal surfaces and directions (Dolan, 338).

$$\frac{dW}{dt} = -\int F_i \dot{x}\, d^3\alpha \quad (7)$$

where

$$F_i = \frac{d}{dx_i}\sqrt{g}\left[\frac{|B|^2}{2\mu_o} + \frac{p}{\gamma - 1} \right] \quad (8)$$

and $\dot{x}_i = (\dot{R},\dot{\lambda},\dot{Z})$ *by use of* $\phi = \zeta$ in the geometric system. Since (8) is a 2nd order differential in flux coordinates, a conservative finite-difference representation is found by integrating (8) over a radial mesh. Spectral analysis of (θ,ζ) is then used so that no higher-order derivatives are computed in the solution of the coupled equations. Equating the magnetic and geometric toroidal angles sets $\partial\phi/\partial\zeta = 0$ and the conservative force equations become

$$F_R = -\frac{\sqrt{g}}{\mu_o}\left[\frac{\partial}{\partial\rho}\left((B^\rho)^2 R_\rho + (B^\rho B^\theta) R_\theta + (B^\rho B^\phi) R_\phi \right) \right. \quad (9a)$$

$$+\frac{\partial}{\partial\theta}\left((B^{\rho}B^{\theta})R_{\rho}+(B^{\theta})^{2}R_{\theta}+(B^{\theta}B^{\phi})R_{\phi}\right)$$
$$+\frac{\partial}{\partial\phi}\left((B^{\rho}B^{\phi})R_{\rho}+(B^{\theta}B^{\phi})R_{\theta}+(B^{\phi})^{2}R_{\phi}\right)\Big]$$
$$+\frac{\partial}{\partial\theta}(PZ_{\rho})-\frac{\partial}{\partial\rho}(PZ_{\rho})-\frac{PG}{R}+\frac{G(RB^{\phi})^{2}}{\mu_{o}}$$

$$F_{\lambda}=-\frac{1}{\mu_{o}}\Big[\frac{\partial}{\partial\phi}(\chi_{\theta}B_{\rho}-\chi_{\rho}B_{\theta})-\frac{\partial}{\partial\rho}(\chi_{\theta}B_{\phi})+\frac{\partial}{\partial\theta}(\chi_{\rho}B_{\phi})\Big] \qquad (9b)$$

with the F_Z equation being symmetric to (9a) except in lacking the last two energy terms and having the R and Z derivatives switched. Note that subscripts on each coordinate denote the first derivative, $G=\sqrt{g}/R$, and $P=R(p+B^2/2\mu_o)$.

Poloidal Flux Profile

For accurate prescription of the poloidal flux, n-degree polynomials in ρ were used as coefficients in a cosine series, represented mathematically as

$$\chi(\rho,\theta)=\chi_{o}(\rho)+\chi_{2}(\rho)\cos(m\theta) \qquad (10)$$

$$where\ \ \chi_{i}(\rho)=\sum_{j=0}^{N}c_{i}^{j}\rho^{j}$$

The number of separatrix X-points is defined by m in (10) and the coefficients are chosen so that the following condition is satisfied:

$$\frac{\partial\chi}{\partial\rho}=\frac{\partial\chi}{\partial\theta}=0 \qquad (11)$$

Noting that when $\theta=0,\pi/2,\pi,3\pi/2\ldots$, then $\partial\chi/\partial\theta=0$. Therefore, the only flux condition defining the polynomial coefficients of the poloidal flux cosine series is

$$\frac{\partial\chi_{o}}{\partial\rho}\pm\frac{\partial\chi_{2}}{\partial\rho}=0\ . \qquad (12)$$

NUMERICAL METHOD

Computational analysis required discretization of the energy principle for numerical integration. Fourier transforms of the

coordinates allow exact interpolation on the half-mesh for more accurate numerical differentiation [9]. Hence, the coordinates are decomposed into even-odd harmonics as

$$\boldsymbol{x}(R,\lambda,Z) = x_{even} + \sqrt{\Delta\rho_{\frac{1}{2}}}\, x_{odd} \tag{13}$$

and averaged onto each nodal point. Following [1] by using central sum and difference formulas on the full-mesh (angular coordinates) and half-mesh (radial coordinate) requires an averaging scheme such that

$$\langle xy \rangle = \left(\frac{x^i y^i + x^{i+1} y^{i+1}}{2} \right) \tag{14}$$

to facilitate higher convergence. However, faster computations could be achieved by averaging the terms separately as $\langle x \rangle \langle y \rangle$. By varying individual nodal amplitudes of the Fourier-transformed force representation, the complete formulation of the steepest-descent algorithm is

$$\frac{\partial X_j^{mn}}{\partial t} = F_j^{mn} \tag{15}$$

Applying (8) as the kernel of the energy integral over all mesh points, averaging onto the full-mesh before differentiation of the energy integral, and decomposing each spatial variable into even and odd components, the Fourier amplitudes may be realized and used to calculate the equilibria solution of minimum plasma energy.

$$R(\rho,\theta,\phi) = \sum_{m,n} R^{mn}(\rho)\cos(m\theta - n\phi) \tag{16a}$$

$$Z(\rho,\theta,\phi) = \sum_{m,n} Z^{mn}(\rho)\sin(m\theta - n\phi) \tag{16b}$$

$$\lambda(\rho,\theta,\phi) = \sum_{m,n} \lambda^{mn}(\rho)\sin(m\theta - n\phi) \tag{16c}$$

NUMERICAL RESULTS

Replication of a standard 3-D MHD equilibria without divertor was easily acquired. Figure 4 illustrates a case in which the modified code successfully solved the MHD equations when the angular dependence was not activated in the poloidal flux (i.e. $\chi(\rho,\theta)=\chi(\rho)$). Shown are the toroidal flux surfaces

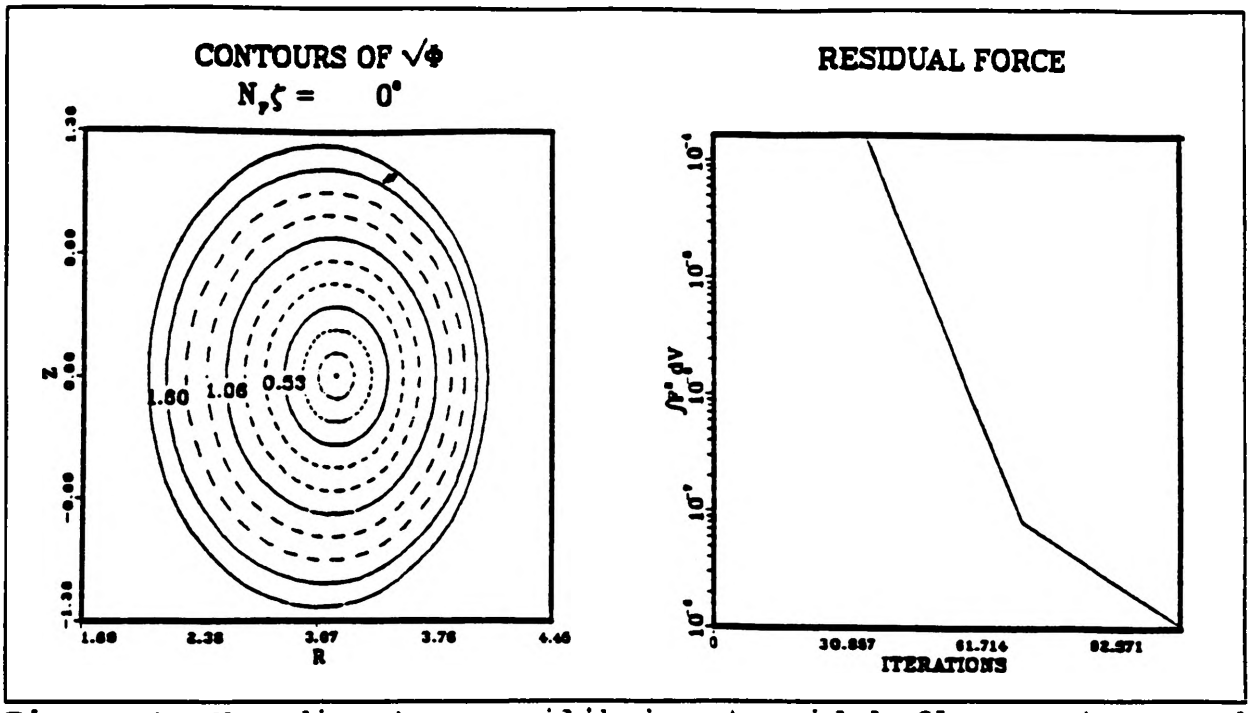

Figure 4. Non-divertor equilibrium toroidal flux contour and residual force decay.

and the residual force going to zero in about 100 iterations. In Figure 5, the angular dependence was "switched" on but the separatrix was not formed within the plasma boundary. The convergence in this case was again adequate.

Two examples of angular-dependent flux profiles in which the X-point is within the plasma boundary are shown in Figures 6 and 7. However, these runs did not converge, even for finer spatial meshes, as is visualized in Figures 8 and 9. The iterative force residual did not smooth out and the magnetic axis (center of ellipsoids) was not resolved.

DISCUSSION

The standard case without divertor was reproducible, as was the case including angular poloidal flux dependence. However, when the separatrix was within the plasma boundary, the residual forces did not decay. This may be due to improper discretization of the energy principle. A finer mesh may improve the convergence properties, but this fact was not seen in any of the cases run here. Analytical derivations are not straightforward and may have led to anomalous errors.

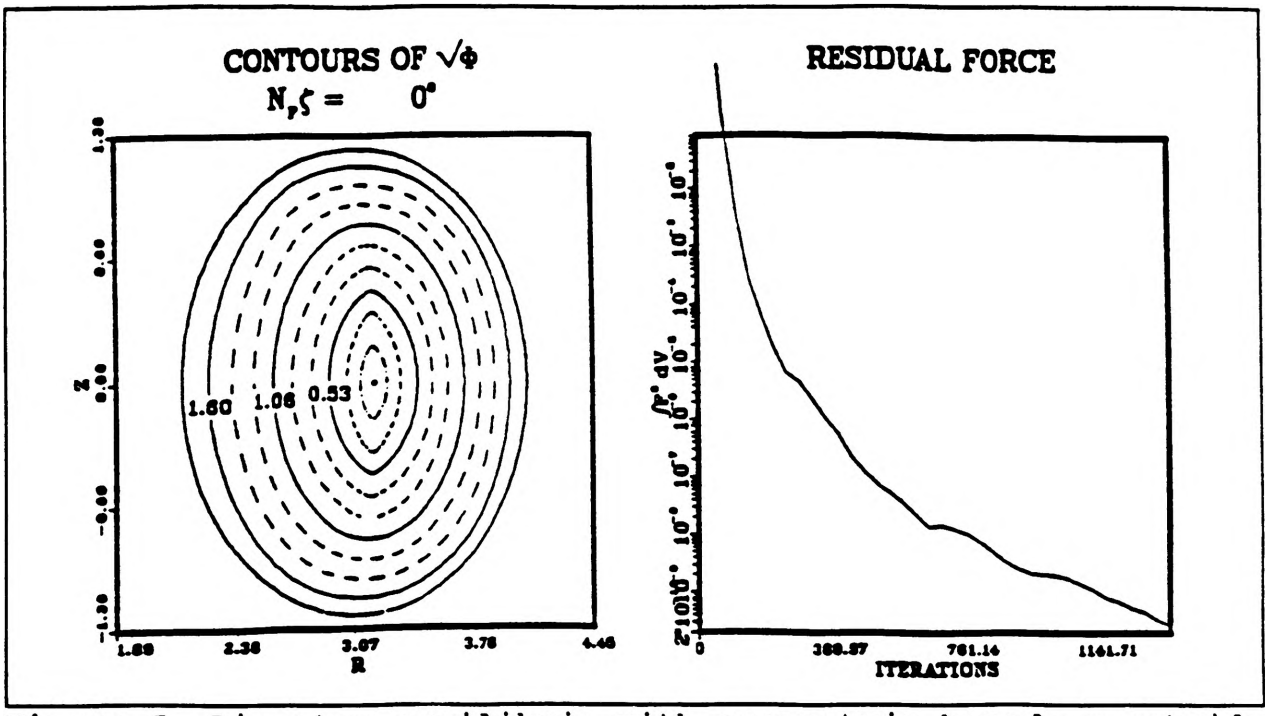

Figure 5. Divertor equilibria with separatrix boundary outside plasma boundary.

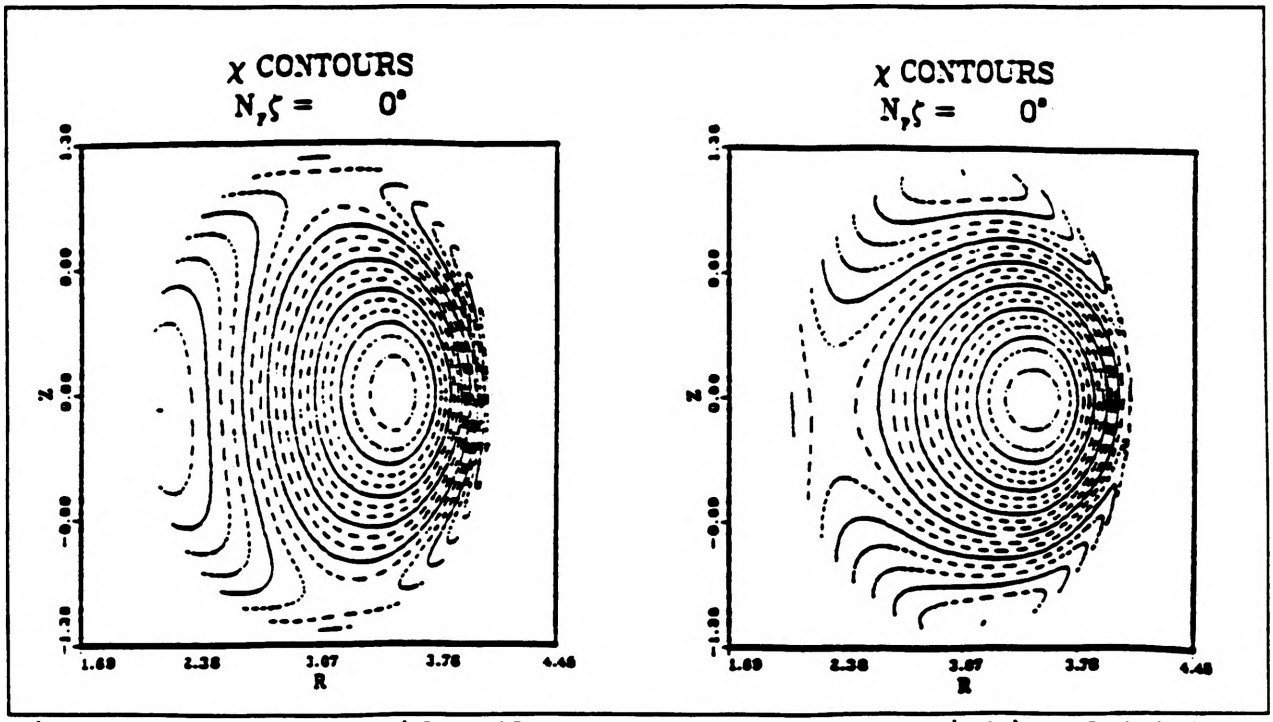

Figure 6(a,b). Poloidal flux surfaces characteristic of (a) top-bottom double-nulled divertor and (b) left (outboard) single-nulled divertor.

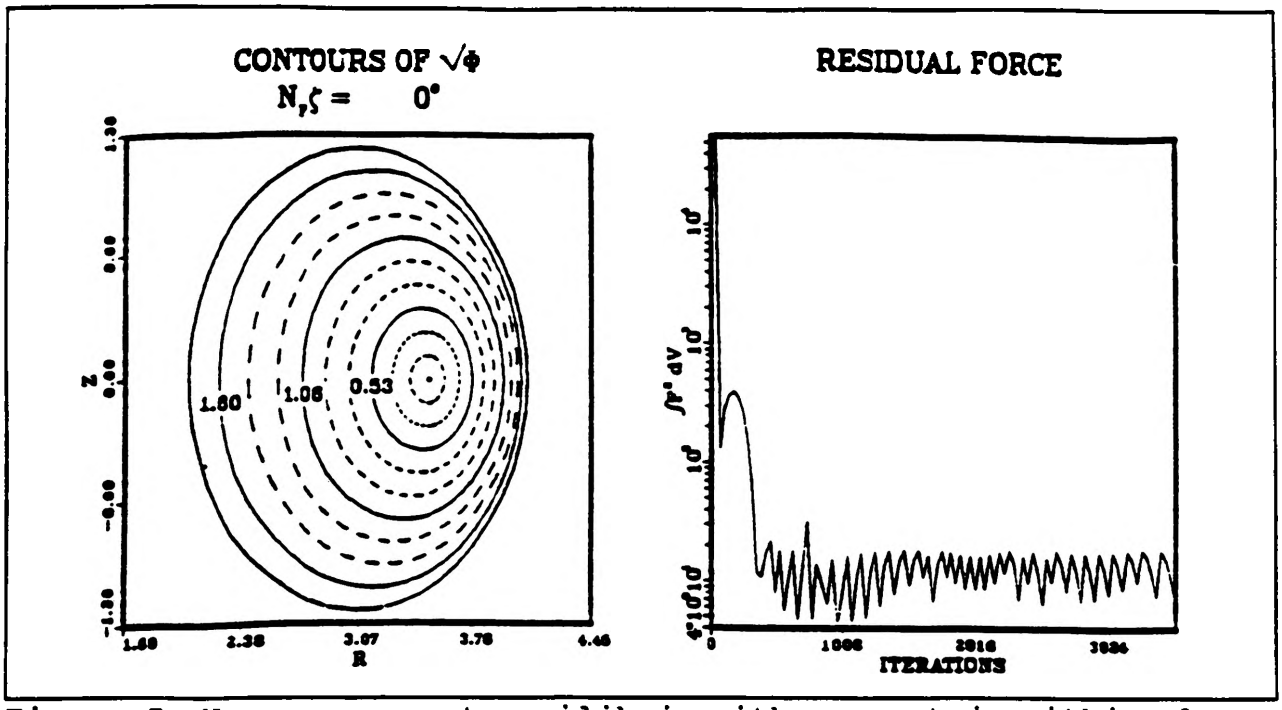

Figure 7. Non-convergent equilibria with separatrix within plasma boundary (number of iterations>1000).

ACKNOWLEDGEMENTS

I would like to thank Dr. Gary Mueller for his helpful guidance and useful conversation. I would also like to thank Steven Hirshman for our insightful discussions. This work was accomplished on a CRAY-2 at the National Magnetic Fusion Energy Computational Center in Lawrence Livermore, California using the Internet and Telnet lines of the Oak Ridge National Laboratory Fusion Energy Division and the UMR Nuclear Engineering AT&T 3B15 mainframe.

REFERENCES

Dolan, T. J. *Fusion Research: Principles, Experiments, & Technology*. Pergamon Press Inc. (1982).

Auerbach, S. P. and Boozer, A. H. "Classical Diffusion in the presence of an X point." Phys. Fluids **23** (1980): 2396-2412.

Boozer, A. H. and Rechester, A. B. "Effect of magnetic perturbations on divertor scrape-off width." Phys. Fluids **21** (1978): 682-689.

Boozer, A. H. "The drift Hamiltonian in a magnetic field with a separatrix." Phys. Fluids B **3** (1991): 875-879.

Hirshman, S. P. and Whitson, J. C. "Steepest-descent moment method for three-dimensional magnetohydrodynamic equilibria." Phys. Fluids **26** (1982): 3552-3568.

Hirshman, S. P., Schwenn, W., and Nuhrenberg, J. "Improved Radial Differencing for Three-Dimensional Magnetohydrodynamic Equilibrium Calculations." J. of Comput. Phys. **87** (1990): 396-407.

Hirshman, S. P. and Betancourt, O. "Preconditioned Descent Algorithm for Rapid Calculations of Magnetohydrodynamic Equilibria." J. of Comput. Phys. **96** (1991): 99-109.

Hirshman, S. P., van Rij, W. I., and Merkel, P. "Three-Dimensional Free Boundary Calculations Using A Spectral Green's Function Method." Computer Physics Communication **43** (1986): 143-155.

Hirshman, S. P. "Curvilinear Coordinates for Magnetic Confinement Geometries." ORNL/TM-8393 Fusion Energy Document (1982).

Kuo-Petravic, G., Boozer, A. H., Rome, J. A., and Fowler, R. H. "Numerical Evaluation of Magnetic Coordinates for Particle Transport Studies in Asymmetric Plasmas." J. of Comput. Phys. **51** (1983): 261-272.